Journal of Contaminant Hydrology 251 (2022) 104068

Contents lists available at ScienceDirect

Journal of Contaminant Hydrology

journal homepage: www.elsevier.com/locate/jconhyd

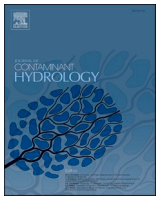

Mass fluxes of dissolved arsenic discharging to the Meghna River are sufficient to account for the mass of arsenic in riverbank sediments

Yibin Huang [a,*], Peter S.K. Knappett [a], Michelle Berube [b], Saugata Datta [c], M. Bayani Cardenas [d], Kimberly A. Rhodes [e], Natasha T. Dimova [f], Imtiaz Choudhury [g], Kazi M. Ahmed [g], Alexander van Geen [h]

[a] Dept. Geology & Geophysics, Texas A&M University, College Station, TX 77843, USA
[b] Dept. Geological Sciences, Kansa State University, Manhattan, KS 66506, USA
[c] Dept. Geological Sciences, The University of Texas, San Antonio, TX 78249, USA
[d] Dept. Geological Sciences, The University of Texas, Austin, TX 78712, USA
[e] Water Management and Hydrological Sciences Program, Texas A&M University, College Station, TX 77843, USA
[f] Dept. Geological Sciences, University of Alabama, Tuscaloosa, AL 35487, USA
[g] Dept. Geology, University of Dhaka, Dhaka 1000, Bangladesh
[h] Lamont-Doherty Earth Observatory of Columbia University, Palisades, NY 10964, USA

ARTICLE INFO

Keywords:
Arsenic
Groundwater discharge
Permeable natural reactive barrier

ABSTRACT

Shallow (<30 m) reducing groundwater commonly contains abundant dissolved arsenic (As) in Bangladesh. We hypothesize that dissolved As in iron (Fe)-rich groundwater discharging to rivers is trapped onto Fe(III)-oxyhydroxides which precipitate in shallow riverbank sediments under the influence of tidal fluctuations. Therefore, the goal of this study is to compare the calculated mass of sediment-bound As that would be sequestered from dissolved groundwater As that discharges through riverbanks of the Meghna River to the observed mass of As trapped within riverbank sediments. To calculate groundwater discharge, a Boussinesq aquifer analytical groundwater flow model was developed and constrained by cyclical seasonal fluctuations in hydraulic heads and river stages observed at three sites along a 13 km reach in central Bangladesh. At all sites, groundwater discharges to the river year-round but most of it passes through an intertidal zone created by ocean tides propagating upstream from the Bay of Bengal in the dry season. The annualized groundwater discharge per unit width at the three sites ranges from 173 to 891 m^2/yr (average 540 m^2/yr). Assuming that riverbanks have been stable since the Brahmaputra River avulsed far away from this area 200 years ago and dissolved As is completely trapped within riverbank sediments, the mass of accumulated sediment As can be calculated by multiplying groundwater discharge by ambient aquifer As concentrations measured in 1969 wells. Across all sites, the range of calculated sediment As concentrations in the riverbank is 78–849 mg/kg, which is higher than the observed concentrations (17–599 mg/kg). This discovery supports the hypothesis that the dissolved As in groundwater discharge to the river is sufficient to account for the observed buried deposits of As along riverbanks.

1. Introduction

An estimated 94–220 million people around the world consume drinking water with arsenic (As) concentrations that exceed the World Health Organization (WHO) guideline of 10 μg/L (Podgorski and Berg, 2020). Chronic consumption of drinking water with As concentrations exceeding the WHO guideline drives higher rates of cardiovascular diseases, cancers and diabetes in adults, raises infant mortality rates and depresses cognitive development in children (Argos et al., 2010; Chen et al., 2011; Navas-Acien et al., 2005; Quansah et al., 2015; Smith et al., 1992; Wasserman et al., 2004). In spite of more than two decades of interventions, >40 million people in Bangladesh continue to consume groundwater over the WHO limit (Ahmad et al., 2018; Jamil et al., 2019).

* Corresponding author.
E-mail addresses: huangyibin123@tamu.edu, knappett@tamu.edu (Y. Huang), berubem@ksu.edu (M. Berube), Saugata.Datta@utsa.edu (S. Datta), cardenas@jsg.utexas.edu (M.B. Cardenas), ntdimova@ua.edu (N.T. Dimova), avangeen@ldeo.columbia.edu (A. van Geen).

https://doi.org/10.1016/j.jconhyd.2022.104068
Received 14 March 2022; Received in revised form 15 August 2022; Accepted 28 August 2022
Available online 2 September 2022

The dissolved As in shallow aquifers (<30 m) in Bangladesh is derived from the dissolution of As-bearing minerals which were eroded from the Himalayas, transported and deposited by the Ganges and Brahmaputra rivers on the Ganges-Brahmaputra-Meghna Delta (GBMD) (Chakraborty et al., 2015; Fendorf et al., 2010; Mcarthur et al., 2001; Smedley and Kinniburgh, 2002). Iron (Fe)-oxyhydroxide minerals, in particular, carry abundant and easily mobilized As (Fendorf et al., 2010; Harvey et al., 2002; Mcarthur et al., 2004; Nickson et al., 2000; Zheng et al., 2004). These are reductively dissolved in the anoxic, organic matter-rich groundwater which prevails in Bangladesh. This leads to the release and reduction of As from $As(V)_2O_5^-$ to $As(III)_2O_3^0$ (roman numerals denote the redox state of As).

In Bangladesh, oxic river water chemically contrasts with the highly reducing shallow groundwater that has abundant dissolved As and Fe(II) (Fendorf et al., 2010; Islam et al., 2000; Van Geen et al., 2003). In the hyporheic zone (HZ), where groundwater and surface water mix, there is a constant replenishment of dissolved oxygen (DO) and dissolved organic matter (DOM) from river water and dissolved Fe(II) from the groundwater. In the process, dissolved Fe(II) is likely oxidized while As absorbs onto the new hydroxide thereby removing As from groundwater that discharges to the river. This creates the potential for As to be removed by sorption to Fe(III)-oxyhydroxides that precipitate within the HZ (Berube et al., 2018; Datta et al., 2009; Jung et al., 2012; Jung et al., 2015). Knowledge of the prevalence of these natural reactive barriers (NRBs) expanded with the discovery of high sediment As concentrations (>700 mg/kg) in shallow riverbank sediments along freshwater bodies including the Meghna River in Bangladesh (Datta et al., 2009; Jung et al., 2015).

Although the ubiquity and efficacy of these NRBs for removing dissolved As discharging to rivers in Bangladesh is still unclear, there is widespread evidence of an NRB-type phenomenon across various stream, river, and estuarine settings. Working along a small mountain stream in Montana that was heavily contaminated by historical mine tailings spills, Nagorski and Moore (1999) found that the pore-waters within the HZ were enriched in dissolved As compared to both the stream water and the adjacent groundwater. Similar layers have been found along the banks of the Cohas Brook in New Hampshire in the United States (Mackay et al., 2014) and the Narayani-Gandak River in Nepal (Johnston et al., 2015). In the Waquoit Bay estuary, in Massachusetts, sediment enriched with As was observed in the subterranean estuary which was defined as the mixing zone within the sediment between fresh groundwater and seawater (Bone et al., 2006; Charette and Sholkovitz, 2002; Charette et al., 2005; Jung et al., 2009). These found that As had accumulated within a layer of Fe or manganese (Mn) oxide minerals with high surface charge density. These studies confirmed that As-trapping on Fe(III)-oxyhydroxides commonly occurs within the steep redox gradient between fresh water rivers and aquifers containing substantial concentrations of dissolved As. The dimensions of this redox gradient depend primarily on the hydraulic conductivity (K) of the sediment, but river stage fluctuations driven by seasons, tides and dam releases expand the size of this zone and the frequency of mixing between oxidizers and reducers, making it more effective at sequestering dissolved Fe(II) and As.

Laboratory experiments have advanced understanding of the impact of redox oscillations on As mobility in the HZ. Parsons et al. (2013) revealed that whereas anoxic conditions mobilize As, repetitive cycling between oxidizing and reducing conditions immobilized progressively more dissolved As. When the Fe(III)-oxyhydroxides are being reductively dissolved, Couture et al. (2015) observed that As sorbed strongly to the remaining sorbent even as it was concurrently (or subsequently) reduced from As(V) to As(III). This experimental evidence suggested that these layers have the potential to retain As even under substantial redox fluctuations. Other minerals besides the surfaces of Fe-oxyhydroxides may also play an important role in sequestering the dissolved As. Phan et al. (2019) demonstrated that under reducing conditions microbial sulfate (SO_4) reduction led to the sequestration of a portion of dissolved As and newly precipitated sulfide minerals such as mackinawite (FeS).

These studies investigated the behavior of As in the HZ and identified factors controlling As mobility across temporal and spatial scales. Brown et al. (2007) demonstrated that the mass flux of dissolved As advected from the aquifer into the stream varied seasonally and spatially along a 88 m reach of a stream adjacent to the abandoned Brinton Arsenic Mine in Virginia. Therefore, it is necessary to quantify the seasonal and spatial variations in groundwater discharge to estimate dissolved As fluxes towards the river. In humid regions, low lying areas and river valleys tend to receive groundwater (Cartwright et al., 2014; Hubbert, 1940; Krause et al., 2007; Larkin and Sharp, 1992; Larsen et al., 2008; Rhodes et al., 2017; Turco et al., 2007). Observed hydraulic heads at several transects of shallow aquifer monitoring wells installed along a 10 km reach of the Meghna River between 2012 and 2015 suggested the Meghna River in the central part of the GBMD generally gains shallow groundwater for most of the year (Berube et al., 2018; Knappett et al., 2016). These studies, however, did not quantify groundwater discharge. A major goal of this study is to quantify the seasonal and spatial variations in groundwater discharge. This facilitates answering the following questions: 1) What is the seasonal and spatial variability of groundwater discharge along the 13 km reach of the Meghna River? 2) What is the annual mass flux of dissolved As that groundwater carries into the HZ via the shallow aquifer? 3) Is the cumulative mass flux of dissolved As over the past 200 years since the Brahmaputra avulsed to the west of Dhaka sufficient to generate the observed enriched sediment As within the HZ (i.e., 100–20,000 mg/kg in Datta et al. (2009), 1–709 mg/kg in Jung et al. (2015) and 17–599 mg/kg in Berube et al. (2018))?

We hypothesized that immobilized aqueous As that was advected towards the river can account for this enriched sediment As. To test this hypothesis, a groundwater flow model constrained by long-term, high frequency observations of hydraulic heads was developed for a seasonally oscillating river boundary. Based on the calculated groundwater discharge and the assumption that the dissolved As can be completely trapped within the riverbank sediments, the expected mass of As that accumulated in riverbank sediments was calculated by multiplying the groundwater discharge by the locally relevant dissolved As concentrations measured in 1969 tubewells screened within the shallow aquifer along a 13 km reach of the Meghna River. Next, these calculated sediment As concentrations were compared to a limited number of observed As concentrations in sediments across the dry season intertidal zone where the majority of the annual groundwater flux discharges to the river.

2. Study area

The study area is a 13 km reach of the Meghna River in central Bangladesh. This reach defines the eastern border of the sub-district (upazila) of Araihazar (Fig. 1a). The distribution of As concentrations in Araihazar has been well characterized owing to 20 years of research by investigators connected to Columbia University's Arsenic Superfund Project, which evaluated the causes and public health outcomes from long-term exposure to As in drinking water (Argos et al., 2010; Van Geen et al., 2014; Van Geen et al., 2003; Wasserman et al., 2004; Zheng et al., 2005). The river is located approximately 25 km east of the capital city Dhaka. Approximately 10 km south of this reach, the Meghna River joins the Padma River which carries the discharge of both the Ganges and Brahmaputra Rivers – two of the largest rivers in Asia. Ocean tides propagate up the Meghna River from the Bay of Bengal driving 12 h (semi-diurnal) and 14 d (neap-spring) fluctuation periods each of approximately 0.6 m in amplitude within the study reach. In addition to the tidal fluctuations, the Meghna River fluctuates seasonally by approximately 4 m with a peak river stage of ~6.5 m above sea level (masl) and a nadir of ~2.5 masl. The wet season extends from May through October, during which the country receives the vast majority of its rainfall. The dry season extends from November through April.

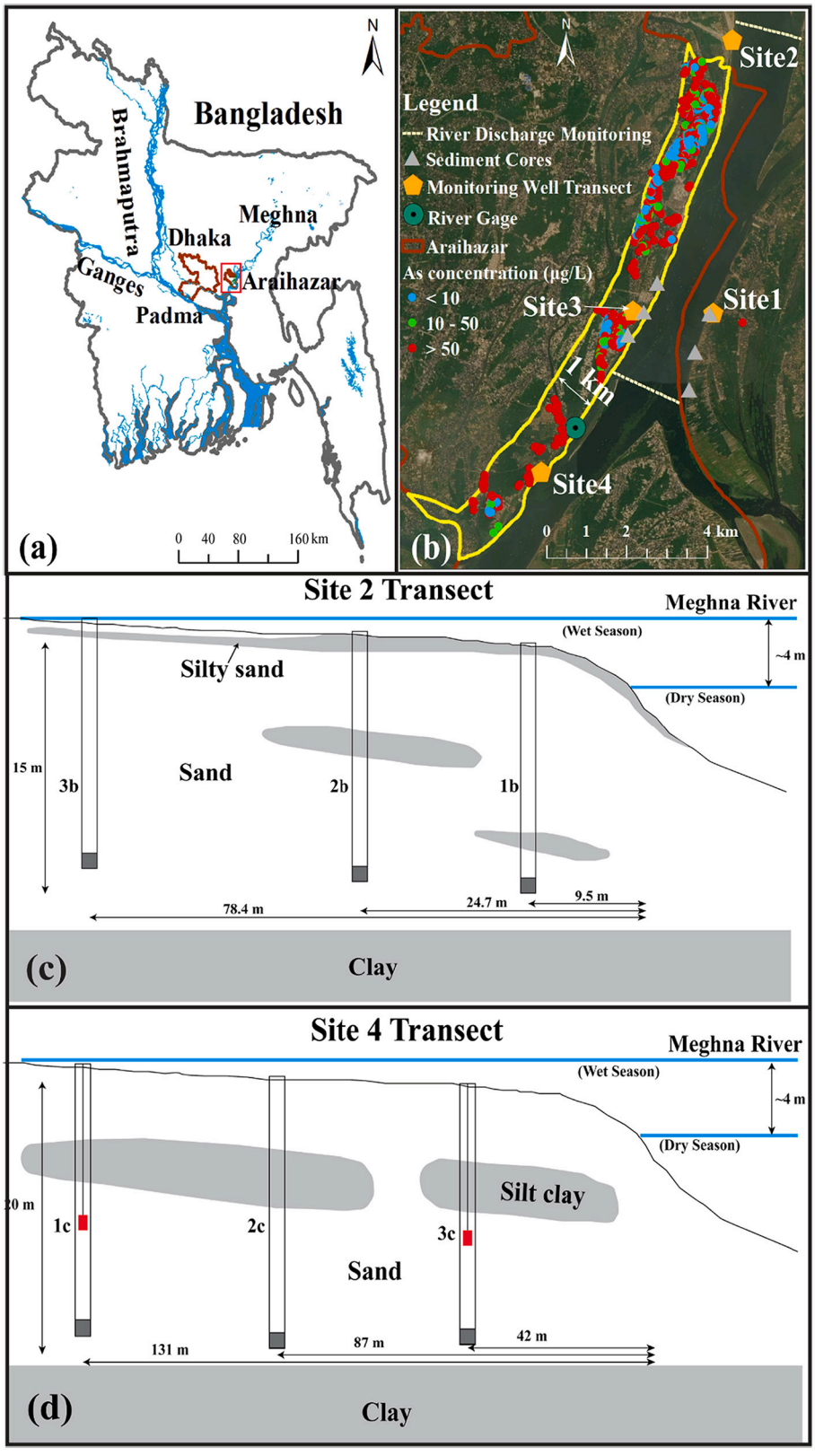

Fig. 1. (a) Location of the study area (red square) within Bangladesh. (b) The 1 km buffer strip (outlined by the yellow solid line) along the Meghna River. Dissolved As concentrations in the shallow aquifer were measured during a blanket survey of wells in Araihazar upazila (Van Geen et al., 2014). The boundary of Araihazar is indicated by the red line. Dashed lines that cross the river indicate the northern and southern locations at which river discharge was measured using an Acoustic Doppler Current Profiler (ADCP). (c) and (d) Vertical profiles of the geology and locations of well screens (gray squares) at S2 and S4, respectively. Red rectangles represent wells that were equipped with pressure transducers for recording hydraulic heads. (For interpretation of the references to colour in this figure legend, the reader is referred to the web version of this article.)

Between 2014 and 2020, four monitoring well transects were installed in the shallow aquifer along the Meghna River to study the fate of As discharging to the river. These are referred to as Sites 1 through 4 (S1-S4) (Fig. 1b). The distribution of monitoring wells that were utilized in this study within S2 and S4 are presented in Fig. 1c and d, respectively. The monitoring wells within transect S1 that were utilized for this study are S1-1a and S1-T5 and were presented in Shuai et al. (2017) and Berube et al. (2018). In S3, only one monitoring well (S3-1a) was screened within the shallow aquifer, which is located approximately 250 m away from the dry season riverbank.

The dimensions of the shallow riverbank aquifer at S1-S4 have been characterized through electrical resistivity tomography (ERT) (Pedrazas et al., 2021; Shuai et al., 2017) and lithological boreholes (Berube et al., 2018; Pedrazas et al., 2021; Shuai et al., 2017). From the ground surface to the depth of ~40 m, there are two main hydro-stratigraphic units: a shallow sandy aquifer that extends to 20–30 m depth; and a clay aquitard with a thickness of 7 m that underlies the shallow aquifer (Berube et al., 2018; Pedrazas et al., 2021; Shuai et al., 2017). The aquifer varies from very fine to coarse sand and the underlying aquitard is blue clay with high plasticity (Berube et al., 2018; Pedrazas et al., 2021). Minor lenses of silty sand and silt were observed at different depths within the aquifer. For example, at S1 and S2, the shallow aquifer is capped by approximately 1 m of silty sand (Pedrazas et al., 2021; Shuai et al., 2017). At S4 (Fig. 1d), there is a laterally extensive silt layer, lying approximately 3 m below land surface with a thickness of 6 m (Pedrazas et al., 2021).

3. Methodology

3.1. Measurements of dissolved and sediment arsenic concentrations

In 2012–13, a blanket survey of As concentrations in private tubewells was completed across Araihazar, in which 48,790 drinking water wells were tested using the ITS Arsenic Econo-Quick kit (https://sensafe.com/quick-arsenic-econo/) (refer to Jameel et al. (2021) for more details). Although the accuracy of the test kit was limited compared with laboratory analysis, the kit reliably categorized As concentrations as being above or below WHO (10 μg/L) and Bangladesh (50 μg/L) drinking water standards (George et al., 2012; Van Geen et al., 2014). A subset of 1,962 wells within the blanket survey with depths shallower than 20 m and located within 1 km from the west bank of the Meghna River shoreline under dry season conditions were utilized to characterize the distribution of dissolved As concentrations in shallow groundwater discharging to the river (Fig. 1b). On the eastern side of the river, Berube et al. (2018) measured groundwater As concentrations within 7 monitoring wells along a transect at S1 with Inductively Coupled Plasma Mass Spectrometer (ICP-MS). Additionally, dissolved Fe was measured in 21 monitoring wells across S1-S4 and 7 private shallow tubewells (Fig. S1 and Table S1). Dissolved Fe concentrations in private tubewells and monitoring wells were measured utilizing a portable spectrophotometer (CHEMetrics, Inc., Midland, VA, USA) (Berube, 2017) and ICP-MS, respectively (Berube et al., 2018).

To investigate As sedimentary concentrations in different groupings of minerals, Berube (2017) performed separate chemical extractions on seven sediment cores collected along the river banks within the study reach (Fig. 1b). Three cores were located on the western side and four on the east (two of them were located at S1). The concentrations of sediment As utilized in the present study were those measured by 1.2 M hydrochloric acid (HCl) extractions which had the highest concentrations of solid-phase As (Berube, 2017). In this extraction procedure, the vast majority of surfaces that the As was attached to were poorly crystallized amorphous Fe(III)-oxyhydroxides and ferrihydrite (Berube, 2017) which sorb As efficiently (Dixit and Hering, 2003).

3.2. Hydraulic properties of the riverbank aquifer

To calculate groundwater discharge, the hydraulic properties of the aquifer need to be measured. Slug tests were performed to measure the spatial variability in K across the aquifer. Duplicate or triplicate measurements were made on each well. Coefficients of variation (C.V.) were typically <2%. Pneumatic rising head slug tests were performed on all monitoring wells in S2 and S3. The pneumatic method was described in Shuai et al. (2017). Solid slug tests were performed on wells in S4 which used a solid slug attached to a pressure transducer utilizing both falling and rising head tests. At all sites, K was calculated using the Hvorslev method (Hvorslev, 1951).

At Site 2, K ranged from 8.8 to 14.5 m/day amongst 4 monitoring wells, with an average of 11.4 m/day and a standard deviation (SD) of 2.6 m/day. At S3, observed K was 111.5 m/day in the single well at that site. At S4, K ranged from 4.3 to 51.6 m/day amongst 9 monitoring wells, with an average of 34.9 m/day and a SD of 14.2 m/day. The value of K at S1 was estimated by Shuai et al. (2017), which conducted both slug and pumping tests at S1. The values of K measured with slug tests ranged from 18.4 to 34.1 m/day amongst 8 monitoring wells with an average of 27.3 m/day and a SD of 5.5 m/day (Shuai et al., 2017). The average value of transmissivity (T) obtained from the pumping tests was 450 m^2/day (Shuai et al., 2017). The thickness of shallow aquifer (b) was 20 m, therefore, the back-calculated K from the pumping tests (T/b) was 22.5 m/day. This falls within the range of K values measured through slug tests indicating the sandy aquifer at that site is relatively homogeneous with respect to K. The full list of the K values is presented in Table S2.

Hydraulic conductivities of the shallow aquifer are available from several field studies throughout Araihazar. In western Araihazar, approximately 10 km west of S3, Stute et al. (2007) and Mozumder et al. (2020a) conducted slug tests on 23 monitoring wells over 7 sites and reported K values ranging from 3.6 to 40.2 m/day, with an average of 17.0 m/day and a SD of 10.9 m/day. Approximately 11 km west of S2, Knappett et al. (2012) conducted slug tests in 50 monitoring wells over 9 transects throughout one village and reported K values ranging from 1.5 to 40.6 m/day with an average of 18.6 m/day and a SD of 11.8 m/day. Therefore, the observed K in the riverbank aquifer sites S1, S2 and S4 are within the range of the inland shallow aquifer but K in the single well in S3 is approximately double the high-end value in 94 previously tested wells throughout the area. Other monitoring wells at S3 within the shallow aquifer were unfortunately not available to further constrain K for this site. Although it is unlikely this high K value is typical of all depths and locations at S3, the presence of this high K layer that is evidently intercepted by the monitoring well will raise the effective K of the entire aquifer even if it is only a few meters thick (Fetter, 2018). Therefore, this value was adopted for the aquifer.

Storativity of the shallow aquifer was reported for several nearby sites in addition to S1 (Mozumder et al., 2020a; Nakaya et al., 2011; Shuai et al., 2017). Based on pumping tests conducted in the shallow aquifer at S1, Shuai et al. (2017) concluded that S was 3.7×10^{-4}. This low value of S combined with the shape of the drawdown curves during the pumping test suggested that this field site is semi-confined, at least in the early dry season when the pumping test was performed. Approximately 10 km west of the S3, Mozumder et al. (2020a) conducted a pumping test in the pre-Holocene aquifer that underlies a 10–15 m thick clay layer that separates it from the overlying Holocene aquifer. They reported that S was 6.2×10^{-4}. Nakaya et al. (2011) used 3×10^{-6} as the value of S for the shallow aquifer located 20 km east of Dhaka which was based on a pumping test. In this study, the value of S derived from Shuai et al. (2017) was adopted in the subsequent analysis to quantify groundwater discharge along both sides of the Meghna River.

3.3. River discharge measurements

Variation in river discharge was measured to compare the magnitude of the calculated groundwater discharge to river discharge during the dry season. Dynamic river discharge during multiple ebb phases of semidiurnal tidal cycles during Jan 4–8, 2015 was measured using an Acoustic Doppler Current Profiler (ADCP; M-9, SonTek/Xylem Inc., San Diego, CA, USA). The ADCP was mounted to the front of a boat using a custom-built aluminum brace (as described in Rhodes et al. (2017)). These measurements were made at northern and southern river cross-section sites which were located approximately 10 km apart and encompassed most of the study area (Fig. 1b). The measurement location alternated each day between the northern and southern river cross-sections. At each location, measurements were made continuously for approximately 6 h. The duration of each river discharge measurement

was approximately 45 min. Therefore, 6–8 measurements were made each day over the course of an ebb tide phase (~8 h).

3.4. Water level measurement and surveying

Pressure transducers (Model 3001, Levelogger Edge, Solinst Canada Ltd., Georgetown, Ontario, Canada) recorded water levels every 20 min in the aquifer and the river. The raw pressures were converted to water table or river stage elevation, as described in Knappett et al. (2016). The distribution of transducers and the corresponding extent of temporal coverage at the river gage and three transects are detailed in Table S3. Only nine months of observations were available at S4, which cannot fully represent the annual fluctuations at this transect. Therefore, records from S4 were extended to twelve months by regressing water table observations at S4 on a simple linear equation that utilized the observed water table at nearby S3. The detailed steps are described in the Text S1 in the Supplementary Material

The elevations of the top of all monitoring wells and river gage were surveyed using repeated real-time kinematic (RTK) surveys with two GPS receivers connected through a radio link (Trimble RTX-Enabled NetR9 and R10, Trimble Inc., Sunnyvale, CA, USA) and on-site surveys with a total station and dumpy level (Berube et al., 2018; Knappett et al., 2016).

3.5. Analytical groundwater flow model

Groundwater discharge across the river-aquifer boundary was quantified by a new analytical solution that was generalizable for both semi-confined and unconfined aquifers. Under the Dupuit assumption, the one-dimensional unsteady groundwater flow in the unconfined aquifer (Fig. 2) is governed by the Boussinesq equation (Bear, 2013; Liang and Zhang, 2012). The governing equation is as follows:

$$K\frac{\partial}{\partial x}\left(h\frac{\partial h}{\partial x}\right)=S_y\frac{\partial h}{\partial t} \tag{1}$$

where K [m/day] is the hydraulic conductivity of the shallow aquifer, x [m] is the horizontal coordinate, h [m] is the hydraulic head in the shallow aquifer with respect to the aquifer bottom, S_y [−] is the specific yield and t [day] is time. Widespread silt or river mud capping on the top of the aquifer is assumed to limit evaporation and infiltration (Berube et al., 2018; Pedrazas et al., 2021). The boundary and initial conditions can be expressed as follows:

$$h(l,t)=u(t) \tag{2}$$

$$h(0,t)=g(t) \tag{3}$$

$$h(x,0)=f(x) \tag{4}$$

where $u(t)$ and $g(t)$ are the time-dependent groundwater level and river stage at the right and left boundaries, respectively (Fig. 2). Both $u(t)$ and $g(t)$ were set equal to observed water levels. $f(x)$ is the initial position of the water table, l is the length of the flow domain, which varies over sites. The term $f(x)$ is the solution to the steady-state solution of $\frac{d}{dx}\left(h\frac{dh}{dx}\right)=0$ and needs to satisfy Eqs. (2) and (3). Therefore,

$$f(x)=\sqrt{g^2(0)+\frac{u^2(0)-g^2(0)}{l}x} \tag{5}$$

3.6. Sediment arsenic estimation

The Ganges and Brahmaputra Rivers combined carry the greatest sediment bedload of all major rivers in the world (Milliman and Meade, 1983; Syvitski and Saito, 2007). This bedload and the avulsions of river channels that its deposition drives, built up the shallow aquifer during the Holocene across the GBMD. During the Holocene, the Brahmaputra River periodically flowed through the subsiding Surma Basin (Acharyya et al., 2000) to the east of the tectonically uplifted Madhupur Tracts in central Bangladesh where the capital city of Dhaka is located (Goodbred et al., 2014) (Fig. 1a). This was the situation in 1770 when the Brahmaputra flowed through Araihazar joining up with the Meghna River (Islam, 2016; Sarker et al., 2003). Around this time the Brahmaputra began to avulse towards the west. This process was completed by 1830 and since then, the Brahmaputra has flown through a similar path to the west of the Madhupur Tracts (Islam, 2016; Sarker et al., 2003). In contrast to the Brahmaputra, the Meghna River is a low-energy river that deposits little new primary sediments downstream of the subsiding Surma Basin which acts like a sediment trap (Rahman et al., 2018). Therefore, to calculate the accumulated mass of As in riverbank sediments, 200 years was implemented in the model which represented the likely time since deposition of the riverbank aquifer sediments. This is an upper time limit for dissolved As to accumulate in riverbank sediments, since scouring and accretion of new sediment on the surficial (<0.3 m) riverbanks does occur during the wet season.

In riverbank sand with moderate permeability, poorly crystalline Fe (III)-oxyhydroxides are hypothesized to precipitate and sequester dissolved As from groundwater discharging to the river. Here we specifically refer to this as a permeable natural reactive barrier (PNRB) (Charette and Sholkovitz, 2002). The term “permeable” distinguishes sandy riverbanks, where advection and dispersion drive mixing, from low permeability estuarine marsh silts where similar Fe(III)-oxyhydroxide deposits have been found but the mixing between oxidants and reductants is driven by molecular diffusion and therefore the scale is smaller (Johnston et al., 2011; Moffett and Gorelick, 2016). In this study, the thickness of the PNRB (H) was obtained from sediment cores collected by Berube (2017). The length of the PNRB (L) was estimated as the ratio of fluctuation of the river stage, which is driven by semi-diurnal and neap-spring tidal cycles, and the grade of the riverbank (Fig. 3). The riverbank grade was estimated using both on-site surveying

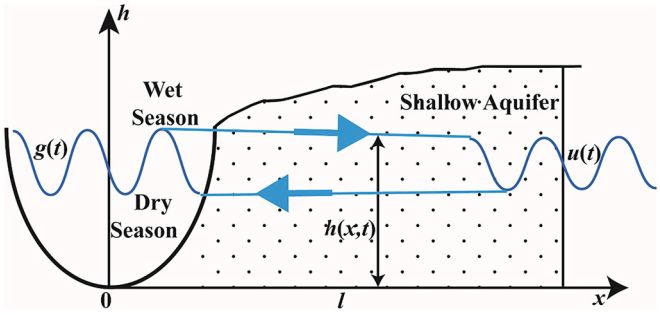

Fig. 2. Schematic diagram representing the periodically fluctuating boundary conditions in the aquifer and river which drive groundwater discharge to the river.

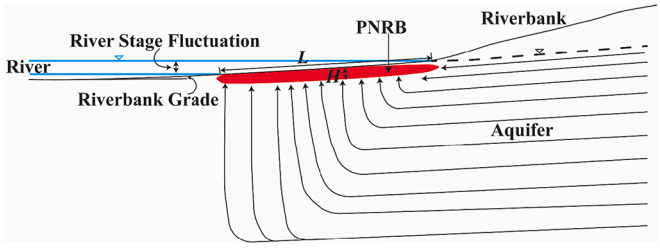

Fig. 3. The conceptual model of groundwater flow paths discharging to the river through the dry season intertidal zone creating the PNRB (red shading). The dry season intertidal zone represents the optimal conditions for the formation of a PNRB owing to the robust semi-diurnal and neap-spring tidal cycles and peak groundwater discharge. (For interpretation of the references to colour in this figure legend, the reader is referred to the web version of this article.)

and the Digital Terrain Elevation Data (DTED) collected by the Shuttle Radar Topography Mission (SRTM) in Google Earth. The riverbanks are broad and largely free of vegetation and these methods gave similar grades.

Hydrological models (Genereux and Bandopadhyay, 2001; Mcbride and Pfannkuch, 1975; Pfannkuch and Winter, 1984; Trefry et al., 2007) predicted that the direction of groundwater flow tends to be vertical near the groundwater-surface water interface. As a result, groundwater discharges through a narrow zone near the shore where the flow paths converge. To estimate the upper limit of accumulated sediment As in PNRB, we assumed that all groundwater discharging to the river passed through the PNRB (Fig. 3) and the dissolved As was completely trapped there (Jung et al., 2015). Based on the above assumptions, the As concentration ($C_{As(s)}$ [mg/kg]) in the riverbank sediment over 200 years was calculated as:

$$C_{As(s)} = 200\left[\frac{QC_{As(aq)}}{1000\rho LH}\right] \tag{6}$$

where Q [m^2/year] is the groundwater discharge per unit width, which was calculated using the analytical groundwater model developed in Section 3.5, $C_{As(aq)}$ [μg/L] is the dissolved As concentration in groundwater, ρ [g/cm^3] is the bulk density, which was assumed to be 2 g/cm^3 (Jung et al., 2015; Mozumder et al., 2020b) and H [m] and L [m] are the thickness and length of PNRB, respectively. Under steady-state conditions with respect to the pore-water chemistry of an aquifer, there is no net retardation of the mass flux of a solute since it is at chemical equilibrium with the sorption sites within a continuous plume (Fetter, 2018). Therefore, there is no retardation term in Eq. 6.

4. Results

4.1. Analytical solution of the groundwater flow boundary value problem

The form of the analytical hydraulic model was chosen for modeling any type of aquifer (confined and unconfined) that is connected to a river with a regularly oscillating stage. The nonlinearity of the governing equation (Eq. (1)) means that it is difficult to obtain its analytical solution except for some special cases. Therefore, Eq. (1) must be linearized and then rewritten as (Bear, 2013; Liang and Zhang, 2012):

$$\beta\frac{\partial^2\Phi}{\partial x^2} = \frac{\partial\Phi}{\partial t} \tag{7}$$

where $\Phi = h^2$ and $\beta = K\overline{h}/S_y$. In the latter term, $\overline{h}$ is the average of the saturated thickness of the aquifer. Assuming that $\Phi(x,t)$ can be written as $\Phi(x,t) = v(x,t) + w(x,t)$, we can derive

$$v(x,t) = \left(1-\frac{x}{L}\right)g^2(t) + \frac{x}{L}u^2(t) \tag{8}$$

$$w(x,t) = -\sum_{n=1}^{\infty}\int_0^t \frac{2u^2(0)}{n\pi}e^{-\alpha t} + \varphi_n(\tau)e^{-\alpha(t-\tau)}d\tau\Big]sin\frac{n\pi}{L}x \tag{9}$$

where

$$\alpha = \beta\left(\frac{n\pi}{L}\right)^2 \tag{10}$$

$$\varphi_n(\tau) = 2[g(t)g'(t) + u(t)u'(t)] \tag{11}$$

The steps for deriving $v(x,t)$, $w(x,t)$ and φ_n are listed Text S2 in the Supporting Information. Once the functions of $g(t)$ and $u(t)$ are obtained and substituted into Eq.'s (8)–(11), the functions of $v(x,t)$ and $w(x,t)$ can be solved, which will derive the function of $\Phi(x,t)$. Then, $h(x,t)$ can be easily calculated by taking the square root of $\Phi(x,t)$.

This study focusses on seasonally changing groundwater discharge between the river and the aquifer. Therefore, the short-term fluctuations of groundwater level and river stage were neglected. The Meghna River fluctuates periodically in a relatively symmetrical way over each year owing to a monsoon season which has a duration of approximately 6 months. Therefore, the river stage and groundwater level at the aquifer boundary can be simulated by simple sine functions ($g(t) = A\sin(Bx + C) + D$ and $u(t) = a\sin(bt + c) + d$). The terms A, B, C, D, a, b, c and d are constants that were fit to the observed river stage and water level, respectively. Then, $h(x,t)$ can be given by

$$h(x,t) = \sqrt{\Phi(x,t)} = \left\{\left(1-\frac{x}{L}\right)[Asin(Bt+C)+D]^2 + \frac{x}{L}[asin(bt+c)+d]^2 - \sum_{n=1}^{\infty}\left[\frac{2(asinc+d)^2}{n\pi}e^{-\alpha t} - \theta(t) - \phi(t)\right]sin\frac{n\pi}{L}x\right\}^{\frac{1}{2}} \tag{12}$$

where

$$\theta(t) = 2A^2BD\frac{B-\alpha}{B^2+\alpha^2}[sin(Bt+C) - cos(Bt+C) - e^{-\alpha t}(sinC - cosC)] - A^2B\frac{2B+\alpha}{4B^2+\alpha^2}[sin(2Bt+2C) + cos(2Bt+2C) + e^{-\alpha t}(sin2C + cos2C)] \tag{13}$$

$$\phi(t) = 2a^2bd\frac{b-\alpha}{b^2+\alpha^2}[sin(bt+c) - cos(bt+c) - e^{-\alpha t}(sinc - cosc)] - a^2b\frac{2b+\alpha}{4b^2+\alpha^2}[sin(2bt+2c) + cos(2bt+2c) + e^{-\alpha t}(sin2c + cos2c)] \tag{14}$$

The groundwater discharge per unit width of the aquifer can be derived by taking the derivative of $h(x,t)$ with respect to x:

$$Q = -Kh\frac{\partial h}{\partial x} = -\frac{K}{2}\frac{\partial\Phi}{\partial x} \tag{15}$$

where Q [m^2/year] is the groundwater discharge per unit width of the aquifer.

4.2. Estimating groundwater discharge

4.2.1. Determining water levels at the model boundaries

Sine functions that represent river stage and groundwater level at the aquifer boundary have to be determined first so they can be input into the Eq. 12. The observed water table in wells S1-1a, S3-1a and S4-1c was used to constrain the aquifer boundary for the separate models from S1, S3 and S4, respectively. The coefficient of determination (R^2) between observed and fitted water levels at aquifer boundaries exceeds 0.94 (Fig. 4) whereas the root mean square error (RMSE) ranges from 0.27 to 0.31 m. This error in the model derived from short-term tidal fluctuations during the dry season or episodic flooding during the wet season. The water table fluctuates ~4 m annually. Thus, the RMSE is approximately 7% of the annual fluctuation which is a minor component.

The relative amounts and timing of monsoon rainfall over the study period have been quite stable. Weekly precipitation amounts measured along one of the two primary tributaries to the Meghna River in Sylhet and in nearby Dhaka between 2014 and 2020 (Fig. S2) both match the

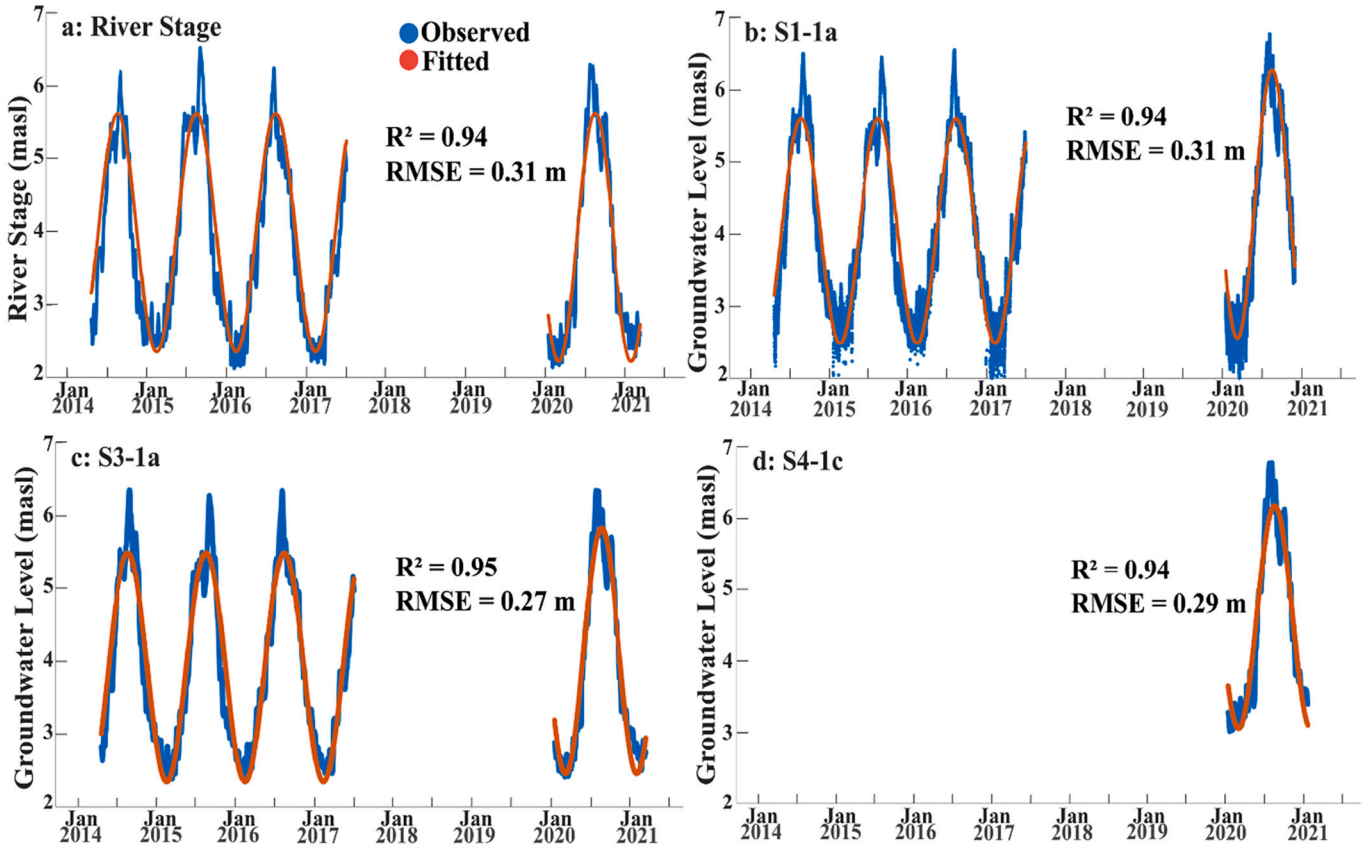

Fig. 4. The observed (blue) and fitted (red) boundary conditions: (a) river stage, (b) – (d) water table at S1-1a, S3-1a and S4-1c, respectively. The coefficient of determination (R^2) and the root mean square error (RMSE) between observed and fitted water level for each monitoring well and river gage are presented. (For interpretation of the references to colour in this figure legend, the reader is referred to the web version of this article.)

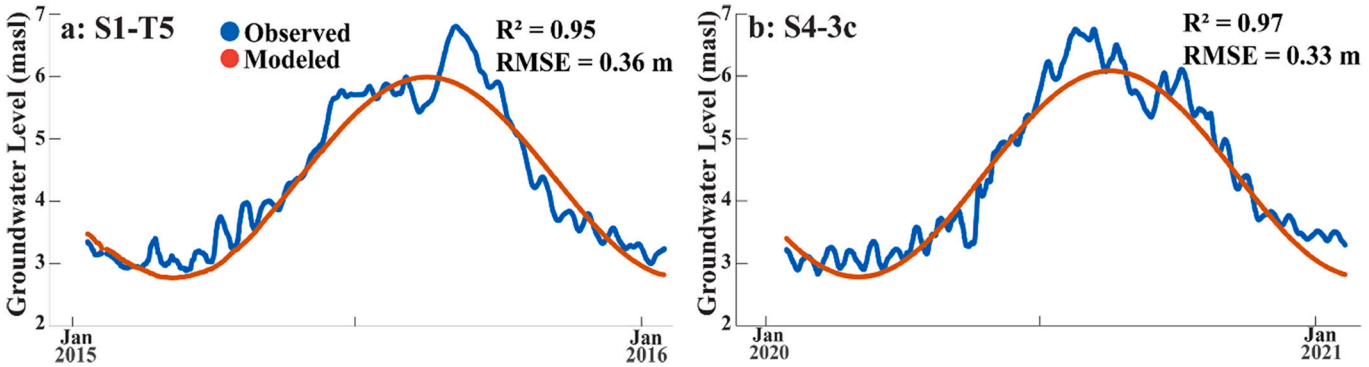

Fig. 5. Model verification by comparing the observed (blue) and modeled (red) water table at (a): S1-T5, (b): S4-3c. (For interpretation of the references to colour in this figure legend, the reader is referred to the web version of this article.)

timing of river stage and water table oscillations. In any given year, the Surma Basin part of the Meghna River watershed receives approximately double the rainfall compared to the study reach (Fig. S3). The stability of recent timing of the monsoon, as well as the total amounts provides evidence of the relative stability of the hydrologic cycle in this region over the past 60 years. This stability is a key assumption in Eq. 6.

4.2.2. Analytical model verification

After fitting the sine functions that best represented water levels at the aquifer and river boundaries, the performance of the model was challenged against independent water level observations that were not used to generate the predicted shape of the water table over time. This was performed for the models at S1 and S4, where a time series of synoptic observations of the water table were available in at least one other monitoring well (S1-T5 and S4-3c). The values of R^2 and RMSE at S1 were 0.95 and 0.36 m, respectively (Fig. 5a). At S4, these corresponding values were 0.97 and 0.33 m, respectively (Fig. 5b). This successful test indicates that the model accurately represents the seasonal fluctuation in the shape of the water table between the known aquifer boundary condition and river stage.

4.2.3. Calculating groundwater discharge through the riverbank

Groundwater discharge was calculated over one year at S1, S3 and S4 (Fig. 6). Negative values indicate water flowing from the aquifer to the river (gaining river). At all sites, the river is gaining groundwater for nearly the entire year. This agrees with observations reported by other

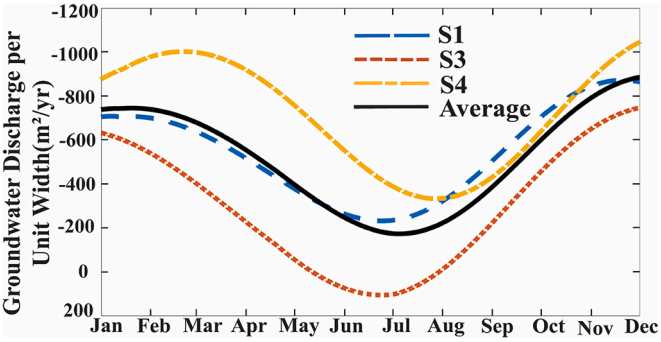

Fig. 6. Modeled groundwater discharge per unit width of the shallow aquifer at sites S1, S3 and S4 and their average. Negative and positive values indicate a gaining and losing river, respectively.

authors studying the seasonally-influenced groundwater discharge to rivers located in low-lying regions (Berube et al., 2018; Krause et al., 2007; Larsen et al., 2008). At S1, groundwater discharge per unit width of the aquifer varied between −233 and − 872 m^2/yr with an average of −562 m^2/yr. Site 3 had the smallest discharge rate, which varied between 104 and − 756 m^2/yr with an average of −318 m^2/yr. At S4, discharge varied between −333 and − 1094 m^2/yr with an average of −754 m^2/yr. Although the specific timing of groundwater discharge variations differed between the three sites, the general shape was similar. The average groundwater discharge (black line in Fig. 6) over the three sites was calculated, which ranged from −173 to −891 m^2/yr with an annualized average of −540 m^2/yr. This average groundwater discharge peaks in January and then reaches a minimum in the early monsoon in July.

Although river discharge during the dry season is highly dynamic over a single semidiurnal tidal cycle (Fig. S4), the relative contribution of groundwater discharge to the river discharge along this study reach is always quite low. During January 2015, river discharge ranged from 150 m^3/s in the upstream direction (north) to 3658 m^3/s in the downstream direction (south) over multiple ebb tides with an average of 2100 m^3/s. For comparison, the average groundwater discharge during the month of January was only 0.6 m^3/s or 0.03% of river discharge.

4.3. Predicting sediment As concentrations within the intertidal zone

4.3.1. Spatial distribution of dissolved As in groundwater

The concentrations of As in 1,962 shallow wells were utilized to represent the distribution of dissolved As in the groundwater along the western bank of the Meghna River. Utilizing the spatial autocorrelation package in ArcGIS 10.8.1 (ESRI, Redlands, CA, USA), a spatial dependence of 350 m was found (Fig. S5). Then, inverse distance weighted (IDW) was used to spatially average dissolved As concentrations over 350 × 350 m^2 squares. Low concentration zones (<50 μg/L) are located in the northern area, whereas high concentration (>200 μg/L) zones are located in the south (Fig. 7). The direction of groundwater flow is generally perpendicular to the riverbank because the hydraulic gradients are large in that direction (Benner et al., 2008; Sun et al., 2016). Therefore, the 1 km buffer strip was divided into 37 rectangular zones oriented parallel to the groundwater flow direction. These were labeled as 1 to 37 from north to south (Fig. 7). Each zone is 350 × 1000 m^2 in size and divided into three 350 × 350 m^2 squares (Fig. 7). For each zone, the dissolved As concentration in groundwater discharging to the river was assumed to be the average of the three square zones along the flow path (Fig. 8a).

On the eastern riverbank, only 7 monitoring wells located within S1 were sampled for the groundwater As concentration. Due to the limited measurements, we were not able to perform the same spatial analysis as we did along the western bank. Therefore, the average dissolved As concentration of the 7 wells was utilized to represent the dissolved As concentrations in groundwater discharging to the river at S1. This is 325 ± 143 μg/L (Fig. 8a).

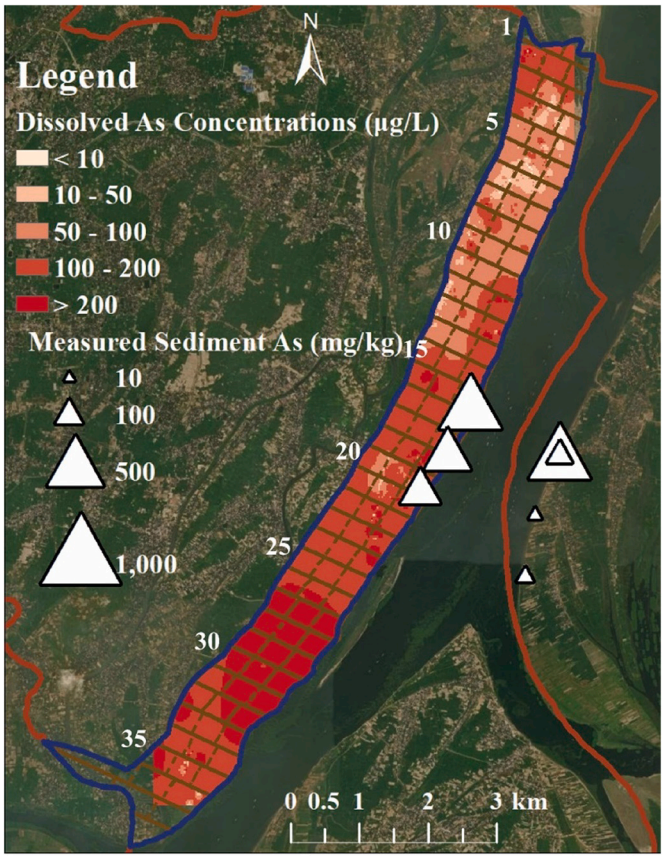

Fig. 7. The contoured area shows the distribution of dissolved As concentrations in shallow groundwater within 1 km buffer strip along the western bank of the Meghna River. The number along the boundary of 1 km buffer strip indicates the ID of each zone.

4.3.2. The dimensions of the intertidal zone and the PNRB

The HCl-extracted sedimentary As concentrations from 7 cores (Fig. 7) suggested that the depth of PNRB was about 1 m (Berube, 2017; Berube et al., 2018). Other authors studying locations 10 km south of the present study area, found evidence of a PNRB at depths of 0–2 m (Jung et al., 2015). Therefore, we adopted 1 m as the thickness of PNRB (*H*) in this study (Fig. 3). Surveying using a total station revealed that the riverbank at S1 has an approximate grade of 7% (Berube et al., 2018). In the dry season, the river stage fluctuates 1.2 m driven by semi-diurnal and neap-spring tidal cycles. Therefore, the length of the PNRB (*L*) at S1 would be 17 m (Fig. 3). Using the same method, the bank grades at S2 and S4 were found to be 3%. Sites 2 and 4 are located in As concentration zones 1 and 31, respectively. Therefore, 3% was assumed to be the representative bank grade of the zone. The riverbank grades near S1, S2 and S4 were also estimated from Google Earth by drawing transects across the bank and extracting elevations from the embedded shuttle radar data. These deviated <1% from the surveyed grades. Thus, Google Earth was utilized to estimate the representative riverbank grades for each zone. These grades are detailed in Table S4. Over 38 zones on the west bank, the riverbank grade varies between 3 and 6%. Based on the 1.2 m total tidal fluctuation amplitudes in river stage, this causes the intertidal zone to range from 19 m to 40 m, with the average of 28 m.

4.3.3. Calculated and measured sediment As concentration in PNRB

Four of seven cores were taken near S1 on the eastern bank (Fig. 7). The average observed sediment As concentrations over 1 m in these

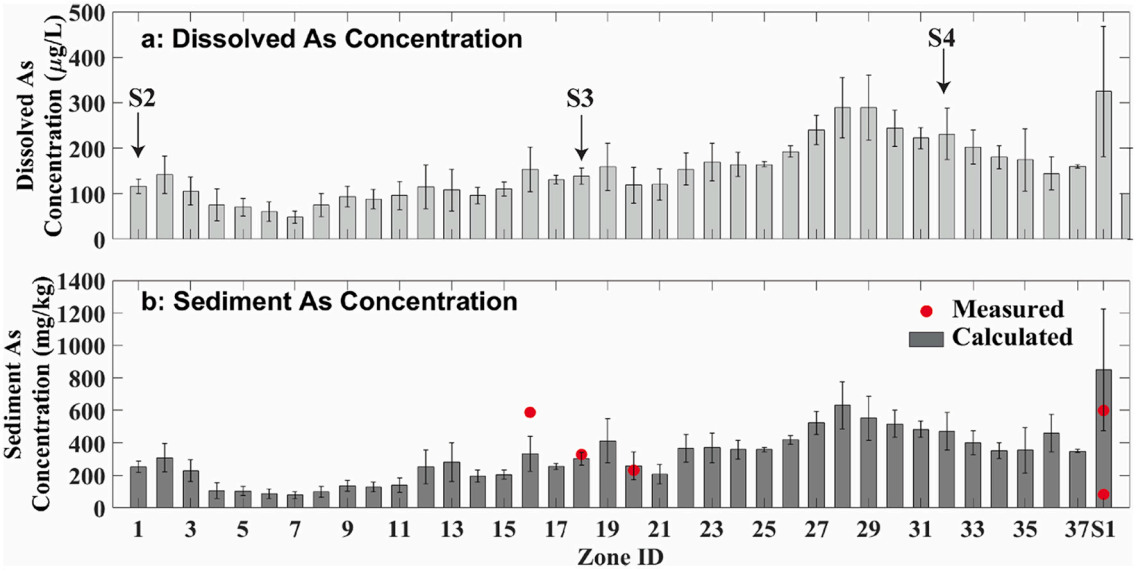

Fig. 8. (a) The average and SD of measured dissolved As concentration in groundwater discharging into the river in each zone. (b) The available measured (red points) and calculated (gray bars) sediment As concentration within the intertidal area in each zone. The S2, S3 and S4 transects are located in zone1, 18 and 31, respectively. Only two sediment cores that were collected near S1 are presented. (For interpretation of the references to colour in this figure legend, the reader is referred to the web version of this article.)

cores were 83, 599, 31 and 17 mg/kg, respectively. The other three cores were located in zones 16, 18 and 20 along the west bank (Fig. 7) and the depth-averaged observed sediment As concentrations were 588, 328 and 231 mg/kg, respectively (Fig. 8b). These measured sediment As concentrations were greatly enriched over values at depths deeper than 1 m at all cores and also hundreds of times greater than the HCl-extractable As found in other high-As shallow aquifer sites throughout Araihazar (1.3–1.5 mg/kg in Radloff et al. (2007) and 0.5–2.9 mg/kg in Zheng et al. (2005)) as well as other nearby sites within the Holocene aquifer (<0.6 mg/kg in Harvey et al. (2002)).

Based on the calculated average groundwater discharge rate over S1, S3 and S4, the estimated dissolved As concentration and the dimensions of PNRB in each zone, the predicted corresponding sediment As concentration was calculated utilizing Eq. 6 (Fig. 8b). Over 37 zones on the western riverbank, zone 28 was predicted to have the highest concentration of 630 ± 144 mg/kg. In contrast, Zone 7 was predicted to have the lowest concentration of 78 ± 21 mg/kg. Observed sediment As concentrations were available at four locations. At zone 16, the observed concentration (588 mg/kg) is somewhat higher than the range of predicted concentration of 334 ± 107 mg/kg (Fig. 8b). In zone 18, however, the observed concentration (328 mg/kg) is close to the predicted concentration of 301 ± 39 mg/kg. The same is true for zone 20. At S1, the observed concentrations from two cores (83 and 599 mg/kg) collected at S1 are within the range of predicted concentration, which is 849 ± 373 mg/kg.

In contrast to the similarity between the predicted and observed sediment As concentrations, far less HCl-extractable Fe was observed within the sediments than predicted based on the 200 year mass fluxes of dissolved Fe (Eq. 6) (Text S3 in the Supporting Information).

5. Discussion

5.1. Seasonal changes in groundwater discharge to the river

In this study, we found that in a low-lying delta with a monsoonal climate, the seasonal variation in groundwater discharge is impacted by the wet and dry seasons. At the beginning of the wet season, the river stage rises faster than the water table. This is the time that the minimum groundwater discharge occurs at all three sites (S1, S3 and S4) (Fig. 6). The interaction between the timing and amounts of precipitation across the Meghna River watershed drives differences in the timing of the rising of river stage and the local water table. Thus, the timing of minimum discharge varies year-to-year (Table S5). Whereas multiple years of water table measurements were made at S1 and S3, at S4 only approximately one-year (2020) of measurements were available. The average timing of the minimum groundwater discharge varied slightly over the three sites.

Groundwater discharge remains low throughout the wet season and then increases throughout the late wet and early dry season when river stage falls quickly while the local water table remains high. During the late dry season (February–April), the local water table converges on the river stage owing to discharge to the river and pumping for agricultural (Harvey et al., 2006) causing flux to decrease.

Some independent measurements are available to compare with these results. Jung et al. (2015) installed 19 seepage meters along the Meghna River in Gazaria upazila (20 km south of the S4) and measured groundwater discharge in the late wet season (Oct 31-Nov 4). During this period, they observed an average groundwater discharge of 22.3 m/day with a SD of 6.6 m/day (Jung et al., 2015). The average groundwater discharge across all sites modeled in this study during the same time of year was 37.7 m/day with a SD of 0.2 m/day.

Even during the early dry season when maximum groundwater discharge occurs, groundwater still only contributed an additional 0.03% to river discharge over the 13 km study reach of this wide, shallow deltaic river (1.5 km wide, 10 m deep) (see Section 4.2.3). This estimate, however, was based on observations and 2-D aquifer models at 3 sites and may have missed much higher transmissivity locations with higher discharge. In general, across lowland rivers, the proportion of groundwater discharge to river discharge varies by season owing to precipitation amounts and intensity, as well as river segment. Poulsen et al. (2015) utilized river-based differential gaging to measure the discharge of a low order stream in Denmark. They observed that baseflow increased the stream discharge from 0.7 to 1.0 m^3/s over the 2.4 km reach, representing a 30% increase. Utilizing differential gaging on the lower Brazos River in central Texas, Rhodes et al. (2017) found that groundwater discharge over a 24 km reach of the lowland river varied from a peak of 15% just after a flood event to zero at the end of a two-month dry period. In contrast, along a 122 km reach of the larger Havel

River in northeastern Germany, differential gaging revealed that annualized groundwater discharge only contributed 0.8 m^3/s or 1% to river discharge (87.9 m^3/s) (Krause et al., 2007). Along a 38 km reach of the Lower Merced River in California, temporal changes in river salinity were utilized to estimate groundwater discharge which was found to contribute <0.1 m^3/s or 0.3–7.0% of river discharge which itself ranged from 1.4 to 31.6 m^3/s (Pai et al., 2015). Together, these findings revealed that baseflow commonly comprised only a small portion of river discharge along higher order, lowland rivers especially during prolonged dry periods. For the Meghna River, the river's discharge during the early dry season likely derives from draining of wetlands across the Surma Basin that are connected with the river and store abundant water during the wet season across the basin (Rahman et al., 2020).

There were some differences in the magnitude and timing of groundwater discharge across the three sites (Fig. 6). At S1 and S4, the direction of groundwater flow was consistently from the aquifer to the river whereas at S3, a minor amount of water flowed from the river to the aquifer between June and July. Moreover, the magnitude of the discharge at S1 and S4 was consistently larger than at S3 despite the high *K* at S3. More groundwater discharged to the river at S4 than S1 during most of the year, but between August and November S4 produced less discharge than S1. Similar patterns in seasonal groundwater discharge have been reported in other studies (Atkinson et al., 2015; Lowry et al., 2007; Poulsen et al., 2015; Taniguchi et al., 2003; Unland et al., 2013).

5.2. Predicted sediment arsenic concentrations and its association with sediment Fe

Except for zone 16, the predicted sediment As concentrations (78–849 mg/kg) calculated by multiplying annual groundwater discharge by the average zonal dissolved As concentration are consistent with or higher than observed (Fig. 8b). In zone 16, the observed concentration is 33% higher than the upper limit of that predicted. Due to the high heterogeneity of dissolved As distribution in shallow groundwater, we may have underestimated the average dissolved As concentration in Zone 16, which may have contributed to the lower predicted sediment As concentration than observed. But, in general, this near-closure of the As mass balance suggests that dissolved As in groundwater is the primary source of the enriched concentrations within the PNRBs. In the future, sediment As concentrations should be measured in other zones along the west side of the riverbank to further challenge the predicted concentrations presented in this paper.

Jung et al. (2015) proposed a similar As accumulation model that can also be used to calculate the expected sediment As concentration in a PNRB that accumulates over a given time period. They assumed that groundwater with an average dissolved As concentration of 100 μg/L, was trapped by the PNRB with a bulk density of 2 g/cm^3. After 200 years' accumulation, sediment As concentration in 1 m thick PNRB would be 101 mg/kg. Applying the assumed dissolved As of 100 μg/L and the PNRB thickness of 1 m to Eq. (6), however, yields an expected concentration of 130–318 mg/kg. The reason for the range of predicted sediment As concentrations is from changes in the length of PNRB which ranges from 19 m to 40 m. The discrepancy between two sets of results is mainly caused by the different groundwater discharge rates. The annual groundwater discharge (10 m/yr) assumed in Jung et al. (2015) was estimated over 5 days (Oct 31-Nov 4) measurements. The calibrated Boussinesq model, however, predicts seasonal variation in groundwater discharge. The estimated annualized discharge rate from this study averaged across all three sites was 25 m/yr. This is what drives the estimated sediment As concentration higher than that of Jung et al. (2015). Given the differences between estimating groundwater discharge from a riverbank along a river at multiple locations using modeled hydraulic heads and river stage, and the more direct, but smaller-scale measurement of groundwater discharge with seepage meters, it is encouraging that the results differ by a factor of about 2.5.

The fact that much less HCl-extractable sediment Fe was found compared to that predicted by Eq. 6 for the S1 and S3 where both dissolved Fe in groundwater and observed sediment Fe were available suggests that the Fe captured within the PNRB is either released to the river or is transformed into more crystalline forms. Evidence of the former process was presented in our previous publication. Berube et al. (2018) showed the active release of Fe from the sediment to pore-waters within the PNRB at S1 during January 2016. Arsenic was not released to pore-waters at this place and time and was thought to re-sorb to remaining Fe-oxyhydroxides. Berube et al. (2018) also showed far higher concentrations of sediment Fe within recalcitrant mineral phases extractable with aqua regia or detected with handheld XRF. This contrasted with As which was found to be predominantly in the HCl-extractable phase. Thus, although much more work needs to be done characterizing the specific mineralogy and associations between Fe and As in riverbank sediments, the current evidence points to As being preferentially associated with amorphous or poorly ordered Fe-oxyhydroxide phases, whereas the Fe itself is both released to the river and re-crystallized.

5.3. Sources of uncertainty in the groundwater discharge estimates

To quantify groundwater discharge and the concentration of sediment As derived from dissolved As in groundwater, several assumptions were made which introduced uncertainty in the quantitative values of our findings. First, we assumed that groundwater completely discharges through the intertidal zone, which is 19–40 m inland from the shoreline of the dry season (Fig. 3). During the wet season, however, the river stage will rise beyond the intertidal zone, which will diminish the discharge of groundwater through it. Based on the observed river stage, the intertidal zone is generally inundated between the end of May and early November (Table S6). During this period, the groundwater discharge accounts for approximate 25% of the annual flux. Therefore, we speculate that the actual percentage of groundwater discharge through the intertidal zone is between 75% and 100%. This would proportionately lower the real mass flux of dissolved As advecting to the intertidal zone in a direct 1:1 manner.

Second, we assumed the riverbank was vertical in the analytical hydraulic model to calculate groundwater discharge. But to calculate the accumulation of dissolved As in the PNRB (Eq. 6), groundwater was assumed to discharge across the gently sloping intertidal zone. This inconsistency may have impacted the results. Along the 13 km river reach, the bank grade is 3–7% (see section 4.3.2). Sharp (1977) suggested it was necessary to consider the sloping geometry in an analytical hydraulic model to accurately quantify water exchange between groundwater and surface water. Doble et al. (2012) found that if the riverbank grade increases from 6% to 15%, the bank infiltration rates and storage volume will increase 98% and 40%, respectively. Therefore, the present study may underestimate the groundwater discharge, which will further underestimate the concentration of sediment As.

Third, the observed groundwater table and river stage were represented by sine functions in the analytical model (Sections 4.1 and 4.2.1). These functions do not represent short-term water level fluctuations (Fig. 4) and may cause a divergence in calculated groundwater discharge from a model that is constrained by observed boundary conditions at finer frequency. To assess the sensitivity of discharge to the frequency of hydraulic head observations at the boundaries, a 3-D numerical model was developed within MODFLOW 2000 which is encoded within the Groundwater Modeling System (GMS) utilizing daily average hydraulic heads. Additionally, for comparison, daily groundwater discharge was calculated with Darcy's Law. The general seasonal pattern of groundwater discharge derived from three approaches is consistent (Fig. S6). Listed from most to least complex models, the average annual groundwater discharge derived from three approaches for the numerical (daily), Boussinesq (sine functions) and Darcy's Law (daily) were: −596, −740 and − 707 m^2/yr, respectively. The least complex model produced

an estimated discharge that lay between the numerical and Boussinesq model.

The reason why Darcy's Law performed similarly to the more complex models that explicitly account for water table storage is the small value of S_y (3.7×10^{-4}) used in the studied riverbank aquifer. When the aquifer has higher S_y and water table storage is important, Darcy's Law will underestimate discharge in both directions and in this case either the Boussinesq or the more complex but flexible numerical model will be needed. The difference in the calculated discharge between the daily discretized numerical and the analytical model suggests that the newly developed analytical model may over-estimate discharge by as much as 23%. The advantage of this model over Darcy's Law is that it can be used to estimate groundwater discharge for any type of the aquifer (confined or unconfined). In general, the advantage of an analytical model over a numerical model is the low computing power, greater transparency and therefore reproducibility between studies, and the lower likelihood of over-fitting observations which can improve the identifiability of the key variables that impact discharge or related reaction processes.

5.4. Dissolved arsenic in groundwater is sufficient to account for sediment arsenic in a PNRB

The buried (>5 m) and surficial (1–2 m) depth sediments with high concentrations of As along the Meghna River have been suggested to be formed from groundwater mixing with oxidized river water (Berube et al., 2018; Datta et al., 2009; Jung et al., 2015). If all the dissolved As that was transported to the riverbank over the past 200 years, since the aquifer-building Brahmaputra River avulsed to the west, was completely trapped within the PNRB, the predicted concentrations of sediment As are consistent with or higher than observed using HCl extractions. This suggests that groundwater mass fluxes provide sufficient As to account for all the As in the mapped PNRBs.

Earlier published studies on sources of dissolved As within a shallow aquifer underlying a parafluvial zone of the Mekong River suggested alternative sources of sediment As along the riverbanks. Polizzotto et al. (2008) proposed that As released from the river-derived floodplain sediments replenishes the dissolved sediment As pool in the aquifer, which was diminished through mobilization and advection through the aquifer to the Mekong River. Postma et al. (2010) found that the river mud has a large pool of reactive Fe(III)-oxyhydroxides with high As content and higher ratio of released As/Fe than aquifer sediments and river sand. Therefore, present-day sediments deposited by a river can be an important contemporary source of dissolved As to aquifers which underlie, or are down hydraulic gradient from, floodplains. Although we were not able to directly verify whether the aforementioned alternative sources exist within parafluvial zones of the study reach, the calculations suggested that dissolved As in groundwater can approximately account for the of the extremely elevated mass of sedimentary As found in the riverbank.

6. Conclusions

This study quantified the relationship between water exchange between an alluvial aquifer and the tidally fluctuating Meghna River, and the accumulation of As at the river-aquifer interface. Groundwater discharge was calculated using a newly developed and calibrated analytical model which describes seasonal and spatial variations in discharge over three sites. The average groundwater discharge per unit width at each of three calibrated sites ranges from −173 to −891 m^2/yr. The average across all three sites is −540 m^2/yr. The negative values indicate that the direction of the flux is consistently from the aquifer to the river. This modeled discharge was multiplied by the average dissolved As concentrations measured within shallow private groundwater wells to calculate the expected concentrations of sediment As in the upper 1 m of the riverbanks if indeed all the dissolved As was captured there over 200 years. These predicted sediment As concentrations are consistent with or higher than those observed. This closure of the mass balance suggests that dissolved As in groundwater discharging to the Meghna River is sufficient to account for the enriched sediment As in a PNRB.

CRediT authorship contribution statement

Yibin Huang: Conceptualization, Software, Validation, Formal analysis, Investigation, Data curation, Writing – original draft, Writing – review & editing. **Peter S.K. Knappett:** Conceptualization, Methodology, Validation, Investigation, Resources, Writing – review & editing, Supervision, Project administration, Funding acquisition. **Michelle Berube:** Investigation, Validation. **Saugata Datta:** Conceptualization, Methodology, Validation, Investigation, Resources, Writing – review & editing, Project administration, Funding acquisition. **M. Bayani Cardenas:** Conceptualization, Methodology, Investigation, Resources, Writing – review & editing, Project administration, Funding acquisition. **Kimberly A. Rhodes:** Validation, Investigation. **Natasha T. Dimova:** Validation, Investigation, Resources, Writing – review & editing. **Imtiaz Choudhury:** Investigation. **Kazi M. Ahmed:** Investigation, Resources. **Alexander van Geen:** Investigation, Resources, Writing – review & editing, Funding acquisition.

Declaration of Competing Interest

The authors declare that they have no known competing financial interests or personal relationships that could have appeared to influence the work reported in this paper.

Acknowledgment

This study was supported by the NSF on grants EAR-1852652 (Peter S. K. Knappett), EAR-1852651 (Saugata Datta) and EAR-1852653 (M. Bayani Cardenas) and NIEHS Superfund Research Program grant P42 ES010349. The authors thank Micaela N. Pedrazas, Cansu Demir, and Kyungwon Kwak for field work assistance. We also thank Madeline Schreiber and another anonymous reviewer for providing constructive feedback on the manuscript.

Appendix A. Supplementary data

Supplementary data to this article can be found online at https://doi.org/10.1016/j.jconhyd.2022.104068.

References

Acharyya, S., Lahiri, S., Raymahashay, B., Bhowmik, A., 2000. Arsenic toxicity of groundwater in parts of the bengal basin in India and Bangladesh: the role of quaternary stratigraphy and holocene sea-level fluctuation. Environ. Geol. 39, 1127–1137.

Ahmad, S.A., Khan, M.H., Haque, M., 2018. Arsenic contamination in groundwater in Bangladesh: implications and challenges for healthcare policy. Risk Management and Healthcare Policy 11, 251–261.

Argos, M., Kalra, T., Rathouz, P.J., Chen, Y., Pierce, B., Parvez, F., Islam, T., Ahmed, A., Rakibuz-Zaman, M., Hasan, R., Sarwar, G., Slavkovich, V., Van Geen, A., Graziano, J., Ahsan, H., 2010. Arsenic exposure from drinking water, and all-cause and chronic-disease mortalities in Bangladesh (heals): a prospective cohort study. Lancet 376, 252–258.

Atkinson, A.P., Cartwright, I., Gilfedder, B., Hofmann, H., Unland, N., Cendon, D.I., Chisari, R., 2015. A multi-tracer approach to quantifying groundwater inflows to an upland river; assessing the influence of variable groundwater chemistry. Hydrol. Process. 29, 1–12.

Bear, J., 2013. Dynamics of Fluids in Porous Media. Courier Corporation.

Benner, S.G., Polizzotto, M.L., Kocar, B.D., Ganguly, S., Phan, K., Ouch, K., Sampson, M., Fendorf, S., 2008. Groundwater flow in an arsenic-contaminated aquifer, mekong delta, Cambodia. Appl. Geochem. 23, 3072–3087.

Berube, M., 2017. Geochemical Controls on Arsenic Release into Groundwaters from Sediments: In Relation to the Natural Reactive Barrier. Master Thesis. Kansas State University.

Berube, M., Jewell, K., Myers, K.D., Knappett, P.S., Shuai, P., Hossain, A., Lipsi, M., Hossain, S., Hossain, A., Aitkenhead-Peterson, J., 2018. The fate of arsenic in

groundwater discharged to the meghna river, Bangladesh. Environ. Chem. 15, 29–45.
Bone, S.E., Gonneea, M.E., Charette, M.A., 2006. Geochemical cycling of arsenic in a coastal aquifer. Environ. Sci. Technol. 40, 3273–3278.
Brown, B.V., Valett, H.M., Schreiber, M.E., 2007. Arsenic transport in groundwater, surface water, and the hyporheic zone of a mine-influenced stream-aquifer system. Water Resour. Res. 43.
Cartwright, I., Hofmann, H., Gilfedder, B., Smyth, B., 2014. Understanding parafluvial exchange and degassing to better quantify groundwater inflows using 222rn: the king river, Southeast Australia. Chem. Geol. 380, 48–60.
Chakraborty, M., Mukherjee, A., Ahmed, K.M., 2015. A review of groundwater arsenic in the bengal basin, Bangladesh and India: from source to sink. Current Pollution Reports 1, 220–247.
Charette, M.A., Sholkovitz, E.R., 2002. Oxidative precipitation of groundwater-derived ferrous iron in the subterranean estuary of a coastal bay. Geophys. Res. Lett. 29 (85-1-85-4).
Charette, M.A., Sholkovitz, E.R., Hansel, C.M., 2005. Trace element cycling in a subterranean estuary: part 1. Geochemistry of the permeable sediments. Geochim. Cosmochim. Acta 69, 2095–2109.
Chen, Y., Graziano, J.H., Parvez, F., Liu, M., Slavkovich, V., Kalra, T., Argos, M., Islam, T., Ahmed, A., Rakibuz-Zaman, M., 2011. Arsenic exposure from drinking water and mortality from cardiovascular disease in Bangladesh: prospective cohort study. BMJ 342.
Couture, R.M., Charlet, L., Markelova, E., Made, B., Parsons, C.T., 2015. On-off mobilization of contaminants in soils during redox oscillations. Environ. Sci. Technol. 49, 3015–3023.
Datta, S., Mailloux, B., Jung, H.B., Hoque, M.A., Stute, M., Ahmed, K.M., Zheng, Y., 2009. Redox trapping of arsenic during groundwater discharge in sediments from the meghna riverbank in Bangladesh. Proc. Natl. Acad. Sci. U. S. A. 106, 16930–16935.
Dixit, S., Hering, J.G., 2003. Comparison of arsenic(v) and arsenic(iii) sorption onto iron oxide minerals: implications for arsenic mobility. Environ. Sci. Technol. 37, 4182–4189.
Doble, R., Brunner, P., Mccallum, J., Cook, P.G., 2012. An analysis of river bank slope and unsaturated flow effects on bank storage. Groundwater 50, 77–86.
Fendorf, S., Michael, H.A., Van Geen, A., 2010. Spatial and temporal variations of groundwater arsenic in south and southeast asia. Science 328, 1123–1127.
Fetter, C.W., 2018. Applied Hydrogeology. Waveland Press.
Genereux, D., Bandopadhyay, I., 2001. Numerical investigation of lake bed seepage patterns: effects of porous medium and lake properties. J. Hydrol. 241, 286–303.
George, C.M., Zheng, Y., Graziano, J.H., Rasul, S.B., Hossain, Z., Mey, J.L., Van Geen, A., 2012. Evaluation of an arsenic test kit for rapid well screening in Bangladesh. Environ. Sci. Technol. 46, 11213–11219.
Goodbred, S.L., Paolo, P.M., Ullah, M.S., Pate, R.D., Khan, S.R., Kuehl, S.A., Singh, S.K., Rahaman, W., 2014. Piecing together the ganges-brahmaputra-meghna river delta: use of sediment provenance to reconstruct the history and interaction of multiple fluvial systems during holocene delta evolution. Bulletin 126, 1495–1510.
Harvey, C.F., Swartz, C.H., Badruzzaman, A.B., Keon-Blute, N., Yu, W., Ali, M.A., Jay, J., Beckie, R., Niedan, V., Brabander, D., Oates, P.M., Ashfaque, K.N., Islam, S., Hemond, H.F., Ahmed, M.F., 2002. Arsenic mobility and groundwater extraction in Bangladesh. Science 298, 1602–1606.
Harvey, C.F., Ashfaque, K.N., Yu, W., Badruzzaman, A., Ali, M.A., Oates, P.M., Michael, H.A., Neumann, R.B., Beckie, R., Islam, S., 2006. Groundwater dynamics and arsenic contamination in Bangladesh. Chem. Geol. 228, 112–136.
Hubbert, M.K., 1940. The theory of ground-water motion. The Journal of Geology 48, 785–944.
Hvorslev, M.J., 1951. Time Lag and Soil Permeability in Ground-Water Observations. Waterways Experiment Station, Corps of Engineers, US Army.
Islam, S.N., 2016. Deltaic floodplains development and wetland ecosystems management in the ganges–brahmaputra–meghna rivers delta in Bangladesh. Sustainable Water Resources Management 2, 237–256.
Islam, M.R., Salminen, R., Lahermo, P.W., 2000. Arsenic and other toxic elemental contamination of groundwater, surface water and soil in Bangladesh and its possible effects on human health. Environ. Geochem. Health 22, 33–53.
Jameel, Y., Mozumder, M.R.H., Van Geen, A., Harvey, C.F., 2021. Well-switching to reduce arsenic exposure in Bangladesh: making the most of inaccurate field kit measurements. GeoHealth 5, 1–19.
Jamil, N.B., Feng, H., Ahmed, K.M., Choudhury, I., Barnwal, P., Van Geen, A., 2019. Effectiveness of different approaches to arsenic mitigation over 18 years in araihazar, Bangladesh: implications for national policy. Environ. Sci. Technol. 53, 5596–5604.
Johnston, S.G., Keene, A.F., Bush, R.T., Burton, E.D., Sullivan, L.A., Isaacson, L., Mcelnea, A.E., Ahern, C.R., Smith, C.D., Powell, B., 2011. Iron geochemical zonation in a tidally inundated acid sulfate soil wetland. Chem. Geol. 280, 257–270.
Johnston, S.G., Diwakar, J., Burton, E.D., 2015. Arsenic solid-phase speciation in an alluvial aquifer system adjacent to the himalayan forehills, Nepal. Chem. Geol. 419, 55–66.
Jung, H.B., Charette, M.A., Zheng, Y., 2009. Field, laboratory, and modeling study of reactive transport of groundwater arsenic in a coastal aquifer. Environ. Sci. Technol. 43, 5333–5338.
Jung, H.B., Bostick, B.C., Zheng, Y., 2012. Field, experimental, and modeling study of arsenic partitioning across a redox transition in a Bangladesh aquifer. Environ. Sci. Technol. 46, 1388–1395.
Jung, H.B., Zheng, Y., Rahman, M.W., Rahman, M.M., Ahmed, K.M., 2015. Redox zonation and oscillation in the hyporheic zone of the ganges-brahmaputra-meghna delta: implications for the fate of groundwater arsenic during discharge. Appl. Geochem. 63, 647–660.
Knappett, P.S., Mckay, L.D., Layton, A., Williams, D.E., Alam, M.J., Huq, M.R., Mey, J., Feighery, J.E., Culligan, P.J., Mailloux, B.J., Zhuang, J., Escamilla, V., Emch, M., Perfect, E., Sayler, G.S., Ahmed, K.M., Van Geen, A., 2012. Implications of fecal bacteria input from latrine-polluted ponds for wells in sandy aquifers. Environ. Sci. Technol. 46, 1361–1370.
Knappett, P.S.K., Mailloux, B.J., Choudhury, I., Khan, M.R., Michael, H.A., Barua, S., Mondal, D.R., Steckler, M.S., Akhter, S.H., Ahmed, K.M., Bostick, B., Harvey, C.F., Shamsudduha, M., Shuai, P., Mihajlov, I., Mozumder, R., Van Geen, A., 2016. Vulnerability of low-arsenic aquifers to municipal pumping in Bangladesh. J. Hydrol. 539, 674–686.
Krause, S., Bronstert, A., Zehe, E., 2007. Groundwater–surface water interactions in a north german lowland floodplain–implications for the river discharge dynamics and riparian water balance. J. Hydrol. 347, 404–417.
Larkin, R.G., Sharp, J.M., 1992. On the relationship between river-basin geomorphology, aquifer hydraulics, and ground-water flow direction in alluvial aquifers. Geol. Soc. Am. Bull. 104, 1608–1620.
Larsen, F., Pham, N.Q., Dang, N.D., Postma, D., Jessen, S., Pham, V.H., Nguyen, T.B., Trieu, H.D., Tran, L.T., Nguyen, H., 2008. Controlling geological and hydrogeological processes in an arsenic contaminated aquifer on the red river flood plain, Vietnam. Appl. Geochem. 23, 3099–3115.
Liang, X., Zhang, Y.K., 2012. Analytical solution for drainage and recession from an unconfined aquifer. Groundwater 50, 793–798.
Lowry, C.S., Walker, J.F., Hunt, R.J., Anderson, M.P., 2007. Identifying spatial variability of groundwater discharge in a wetland stream using a distributed temperature sensor. Water Resour. Res. 43.
Mackay, A.A., Gan, P., Yu, R., Smets, B.F., 2014. Seasonal arsenic accumulation in stream sediments at a groundwater discharge zone. Environ. Sci. Technol. 48, 920–929.
Mcarthur, J.M., Ravenscroft, P., Safiulla, S., Thirlwall, M.F., 2001. Arsenic in groundwater: testing pollution mechanisms for sedimentary aquifers in Bangladesh. Water Resour. Res. 37, 109–117.
Mcarthur, J., Banerjee, D., Hudson-Edwards, K., Mishra, R., Purohit, R., Ravenscroft, P., Cronin, A., Howarth, R., Chatterjee, A., Talukder, T., 2004. Natural organic matter in sedimentary basins and its relation to arsenic in anoxic ground water: the example of West Bengal and its worldwide implications. Appl. Geochem. 19, 1255–1293.
Mcbride, M., Pfannkuch, H., 1975. The distribution of seepage within lakebeds. J. Res. US Geol. Surv. 3, 505–512.
Milliman, J.D., Meade, R.H., 1983. World-wide delivery of river sediment to the oceans. The Journal of Geology 91, 1–21.
Moffett, K.B., Gorelick, S.M., 2016. Relating salt marsh pore water geochemistry patterns to vegetation zones and hydrologic influences. Water Resour. Res. 52, 1729–1745.
Mozumder, M., Michael, H., Mihajlov, I., Khan, M., Knappett, P., Bostick, B., Mailloux, B., Ahmed, K., Choudhury, I., Koffman, T., 2020a. Origin of groundwater arsenic in a rural pleistocene aquifer in Bangladesh depressurized by distal municipal pumping. Water Resour. Res. 56, 1–26.
Mozumder, M.R.H., Bostick, B.C., Selim, M., Islam, M.A., Shoenfelt, E.M., Ellis, T., Mailloux, B.J., Choudhury, I., Ahmed, K.M., Van Geen, A., 2020b. Similar retardation of arsenic in gray holocene and orange pleistocene sediments: evidence from field-based column experiments in Bangladesh. Water Res. 183, 116081.
Nagorski, S.A., Moore, J.N., 1999. Arsenic mobilization in the hyporheic zone of a contaminated stream. Water Resour. Res. 35, 3441–3450.
Nakaya, S., Natsume, H., Masuda, H., Mitamura, M., Biswas, D.K., Seddique, A.A., 2011. Effect of groundwater flow on forming arsenic contaminated groundwater in sonargaon, Bangladesh. J. Hydrol. 409, 724–736.
Navas-Acien, A., Sharrett, A.R., Silbergeld, E.K., Schwartz, B.S., Nachman, K.E., Burke, T. A., Guallar, E., 2005. Arsenic exposure and cardiovascular disease: a systematic review of the epidemiologic evidence. Am. J. Epidemiol. 162, 1037–1049.
Nickson, R.T., Mcarthur, J.M., Ravenscroft, P., Burgess, W.G., Ahmed, K.M., 2000. Mechanism of arsenic release to groundwater, Bangladesh and West Bengal. Appl. Geochem. 15, 403–413.
Pai, H., Villamizar, S.R., Harmon, T.C., 2015. High resolution synoptic salinity mapping to identify groundwater–surface water discharges in lowland rivers. Environ. Sci. Technol. 49, 4842–4850.
Parsons, C.T., Couture, R.M., Omoregie, E.O., Bardelli, F., Greneche, J.M., Roman-Ross, G., Charlet, L., 2013. The impact of oscillating redox conditions: arsenic immobilisation in contaminated calcareous floodplain soils. Environ. Pollut. 178, 254–263.
Pedrazas, M.N., Cardenas, M.B., Hosain, A., Demir, C., Ahmed, K.M., Akhter, S.H., Wang, L., Datta, S., Knappett, P.S., 2021. Application of electrical resistivity to map the stratigraphy and salinity of fluvio-deltaic aquifers: case studies from Bangladesh that reveal benefits and pitfalls. Hydrogeol. J. 29, 1601–1610.
Pfannkuch, H., Winter, T., 1984. Effect of anisotropy and groundwater system geometry on seepage through lakebeds: 1. Analog and dimensional analysis. J. Hydrol. 75, 213–237.
Phan, V.T.H., Bernier-Latmani, R., Tisserand, D., Bardelli, F., Le Pape, P., Frutschi, M., Gehin, A., Couture, R.M., Charlet, L., 2019. As release under the microbial sulfate reduction during redox oscillations in the upper mekong delta aquifers, Vietnam: a mechanistic study. Sci. Total Environ. 663, 718–730.
Podgorski, J., Berg, M., 2020. Global threat of arsenic in groundwater. Science 368, 845–850.
Polizzotto, M.L., Kocar, B.D., Benner, S.G., Sampson, M., Fendorf, S., 2008. Near-surface wetland sediments as a source of arsenic release to ground water in asia. Nature 454, 505–508.
Postma, D., Jessen, S., Hue, N.T.M., Duc, M.T., Koch, C.B., Viet, P.H., Nhan, P.Q., Larsen, F., 2010. Mobilization of arsenic and iron from red river floodplain sediments, Vietnam. Geochim. Cosmochim. Acta 74, 3367–3381.

Poulsen, J., Sebok, E., Duque, C., Tetzlaff, D., Engesgaard, P., 2015. Detecting groundwater discharge dynamics from point-to-catchment scale in a lowland stream: combining hydraulic and tracer methods. Hydrol. Earth Syst. Sci. 19, 1871–1886.
Quansah, R., Armah, F.A., Essumang, D.K., Luginaah, I., Clarke, E., Marfoh, K., Cobbina, S.J., Nketiah-Amponsah, E., Namujju, P.B., Obiri, S., 2015. Association of arsenic with adverse pregnancy outcomes/infant mortality: a systematic review and meta-analysis. Environ. Health Perspect. 123, 412–421.
Radloff, K.A., Cheng, Z., Rahman, M.W., Ahmed, K.M., Mailloux, B.J., Juhl, A.R., Schlosser, P., Van Geen, A., 2007. Mobilization of arsenic during one-year incubations of grey aquifer sands from araihazar, Bangladesh. Environ. Sci. Technol. 41, 3639–3645.
Rahman, M., Dustegir, M., Karim, R., Haque, A., Nicholls, R.J., Darby, S.E., Nakagawa, H., Hossain, M., Dunn, F.E., Akter, M., 2018. Recent sediment flux to the ganges-brahmaputra-meghna delta system. Sci. Total Environ. 643, 1054–1064.
Rahman, M.M., Thompson, J.R., Flower, R.J., 2020. Hydrological impacts of climate change on rice cultivated riparian wetlands in the upper meghna river basin (Bangladesh and India). Hydrol. Sci. J. 65, 33–56.
Rhodes, K.A., Proffitt, T., Rowley, T., Knappett, P.S., Montiel, D., Dimova, N., Tebo, D., Miller, G.R., 2017. The importance of bank storage in supplying baseflow to rivers flowing through compartmentalized, alluvial aquifers. Water Resour. Res. 53, 10539–10557.
Sarker, M.H., Huque, I., Alam, M., Koudstaal, R., 2003. Rivers, chars and char dwellers of Bangladesh. International Journal of River Basin Management 1, 61–80.
Sharp, J.M., 1977. Limitations of bank-storage model assumptions. J. Hydrol. 35, 31–47.
Shuai, P., Knappett, P.S.K., Hossain, S., Hosain, A., Rhodes, K., Ahmed, K.M., Cardenas, M.B., 2017. The impact of the degree of aquifer confinement and anisotropy on tidal pulse propagation. Groundwater 55, 519–531.
Smedley, P.L., Kinniburgh, D.G., 2002. A review of the source, behaviour and distribution of arsenic in natural waters. Appl. Geochem. 17, 517–568.
Smith, A.H., Hopenhayn-Rich, C., Bates, M.N., Goeden, H.M., Hertz-Picciotto, I., Duggan, H.M., Wood, R., Kosnett, M.J., Smith, M.T., 1992. Cancer risks from arsenic in drinking water. Environ. Health Perspect. 97, 259–267.
Stute, M., Zheng, Y., Schlosser, P., Horneman, A., Dhar, R., Datta, S., Hoque, M., Seddique, A., Shamsudduha, M., Ahmed, K., 2007. Hydrological control of as concentrations in Bangladesh groundwater. Water Resour. Res. 43.
Sun, X., Bernard-Jannin, L., Garneau, C., Volk, M., Arnold, J.G., Srinivasan, R., Sauvage, S., Sánchez-Pérez, J.-M., 2016. Improved simulation of river water and groundwater exchange in an alluvial plain using the swat model. Hydrol. Process. 30, 187–202.
Syvitski, J.P., Saito, Y., 2007. Morphodynamics of deltas under the influence of humans. Glob. Planet. Chang. 57, 261–282.
Taniguchi, M., Burnett, W.C., Smith, C.F., Paulsen, R.J., O'rourke, D., Krupa, S.L., Christoff, J.L., 2003. Spatial and temporal distributions of submarine groundwater discharge rates obtained from various types of seepage meters at a site in the northeastern gulf of mexico. Biogeochemistry 66, 35–53.
Trefry, M., Svensson, T., Davis, G., 2007. Hypoaigic influences on groundwater flux to a seasonally saline river. J. Hydrol. 335, 330–353.
Turco, M.J., East, J.W., Milburn, M.S., 2007. Base Flow (1966–2005) and Streamflow Gain and Loss (2006) of the Brazos River, Mclennan County to Fort Bend County, Texas. US Geological Survey.
Unland, N., Cartwright, I., Andersen, M.S., Rau, G.C., Reed, J., Gilfedder, B., Atkinson, A. P., Hofmann, H., 2013. Investigating the spatio-temporal variability in groundwater and surface water interactions: a multi-technique approach. Hydrol. Earth Syst. Sci. 17, 3437–3453.
Van Geen, A., Zheng, Y.-J., Versteeg, R., Stute, M., Horneman, A., Dhar, R., Steckler, M., Gelman, A., Small, C., Ahsan, H., 2003. Spatial variability of arsenic in 6000 tube wells in a 25 km2 area of Bangladesh. Water Resour. Res. 39.
Van Geen, A., Ahmed, E.B., Pitcher, L., Mey, J.L., Ahsan, H., Graziano, J.H., Ahmed, K. M., 2014. Comparison of two blanket surveys of arsenic in tubewells conducted 12 years apart in a 25 km2 area of Bangladesh. Sci. Total Environ. 488, 484–492.
Wasserman, G.A., Liu, X., Parvez, F., Ahsan, H., Factor-Litvak, P., Van Geen, A., Slavkovich, V., Loiacono, N.J., Cheng, Z., Hussain, I., Momotaj, H., Graziano, J.H., 2004. Water arsenic exposure and children's intellectual function in araihazar, Bangladesh. Environ. Health Perspect. 112, 1329–1333.
Zheng, Y., Stute, M., Van Geen, A., Gavrieli, I., Dhar, R., Simpson, H., Schlosser, P., Ahmed, K., 2004. Redox control of arsenic mobilization in Bangladesh groundwater. Appl. Geochem. 19, 201–214.
Zheng, Y., Van Geen, A., Stute, M., Dhar, R., Mo, Z., Cheng, Z., Horneman, A., Gavrieli, I., Simpson, H., Versteeg, R., 2005. Geochemical and hydrogeological contrasts between shallow and deeper aquifers in two villages of araihazar, Bangladesh: implications for deeper aquifers as drinking water sources. Geochim. Cosmochim. Acta 69, 5203–5218.